Supplementary Information: Accurate Evaluation on the Interactions of SARS-CoV-2 with its Receptor ACE2 and Antibodies CR3022/CB6

Hong-ming Ding(丁泓铭)[1,*], Yue-wen Yin(尹跃文)[1], Song-di Ni(倪崧荻)[1], Yan-jing Sheng(盛艳静)[1], and Yu-qiang Ma(马余强)[2,*]

[1] Center for Soft Condensed Matter Physics and Interdisciplinary Research, School of Physical Science and Technology, Soochow University, Suzhou 215006, China

[2] National Laboratory of Solid State Microstructures and Department of Physics, Collaborative Innovation Center of Advanced Microstructures, Nanjing University, Nanjing 210093, China

*Email: dinghm@suda.edu.cn, myqiang@nju.edu.cn

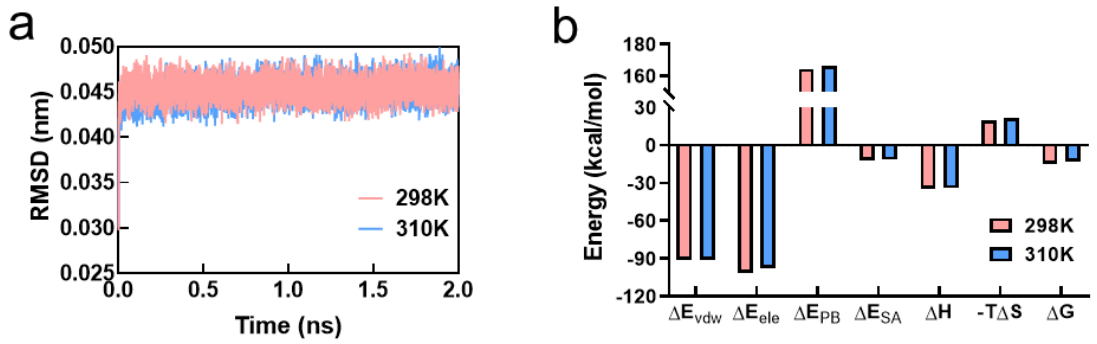

Figure S1. The effect of the temperature on the binding affinity. (a) The root mean square distance (RMSD) of the backbone atoms in the proteins as a function of time at 298K and 310K. (b) The binding free energy and the energy term at 298K and 310K.

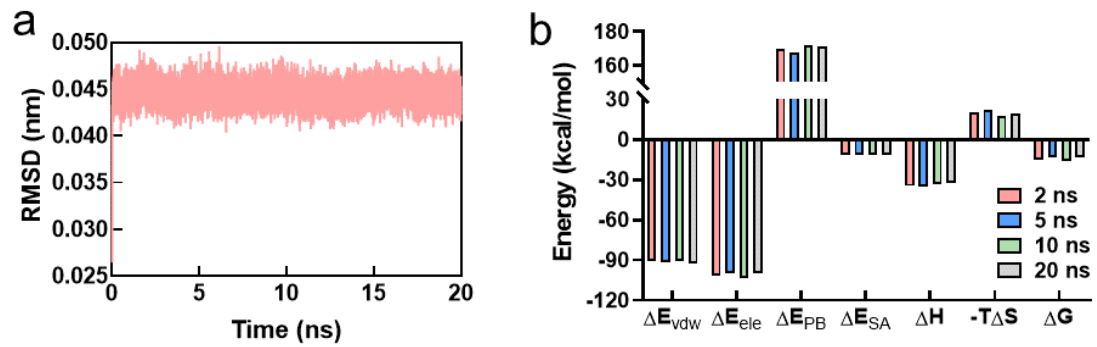

Figure S2. The effect of the time length on the binding affinity. (a) The root mean square distance

(RMSD) of the backbone atoms in the proteins as a function of time. (b) The binding free energy and the energy term as a function of time.

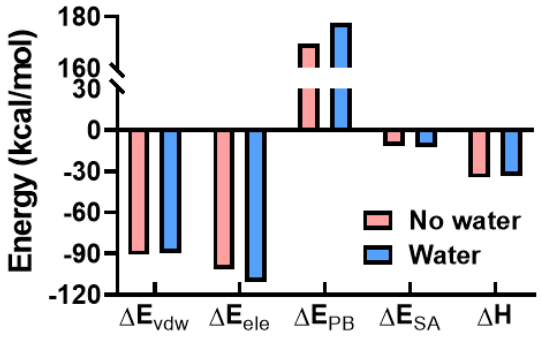

Figure S3. Effect of the water molecule on the binding affinity of SARS-CoV-2 and ACE2. The comparison of binding energy in the presence and absence of associated water molecules at the binding site. For the sake of simplicity, the entropy term is not considered due to the variance of the water molecules at the binding site.

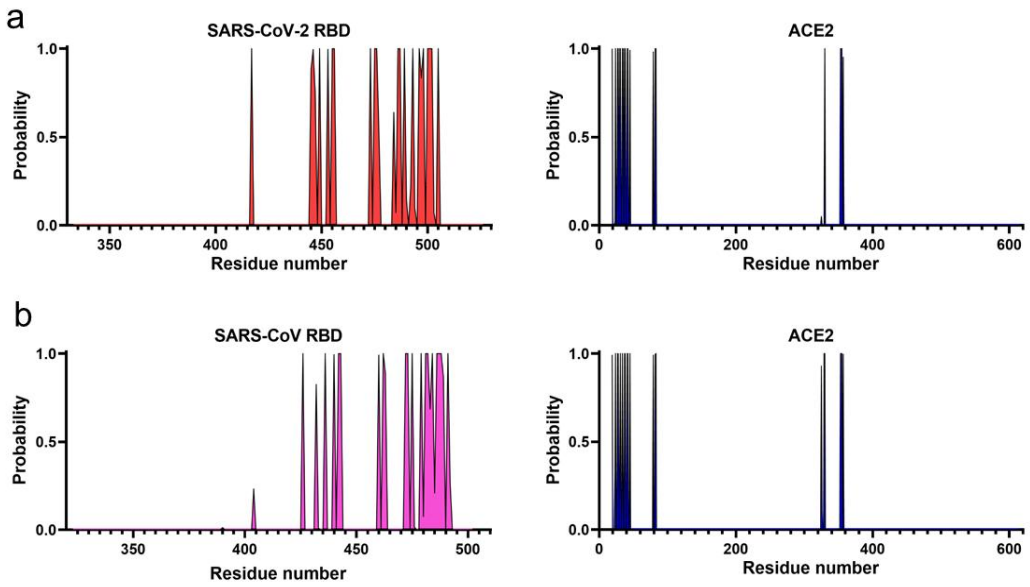

Figure S4. The contact probability of the residues in the SARS-CoV-2 RBD/ACE2 interface (a) and SARS-CoV RBD/ACE2 interface (b). The criterion for the residue contact is that the distance between two heavy atoms is smaller than 0.50 nm.

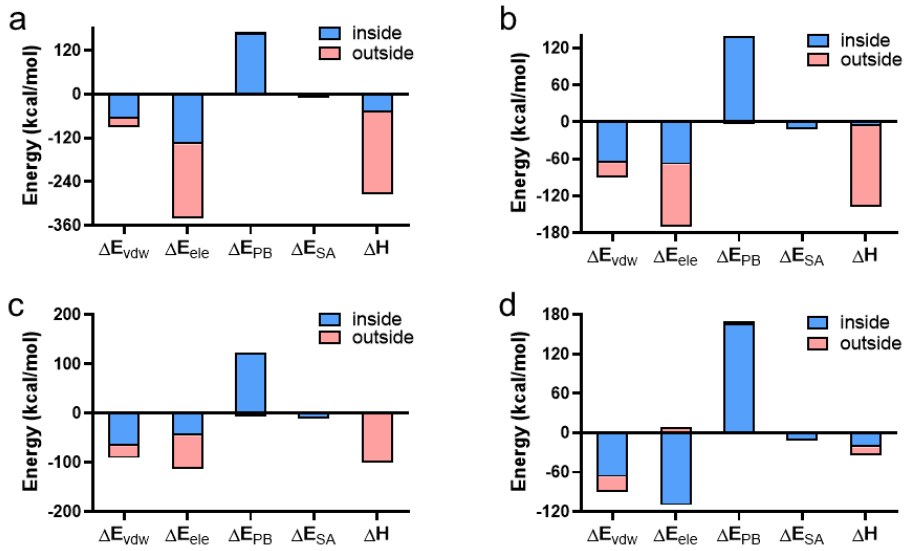

Figure S5. The comparison of the binding energy inside/outside the binding site between the standard MM/PBSA and the screening MM/PBSA. For the sake of simplicity, the entropic term was not considered. (a) Standard MM/PBSA at ε_{in}=2.0, (b) standard MM/PBSA at ε_{in}=4.0, (c) standard MM/PBSA at ε_{in}=6.0, (d) screening MM/PBSA at ε_{in}=2.0.

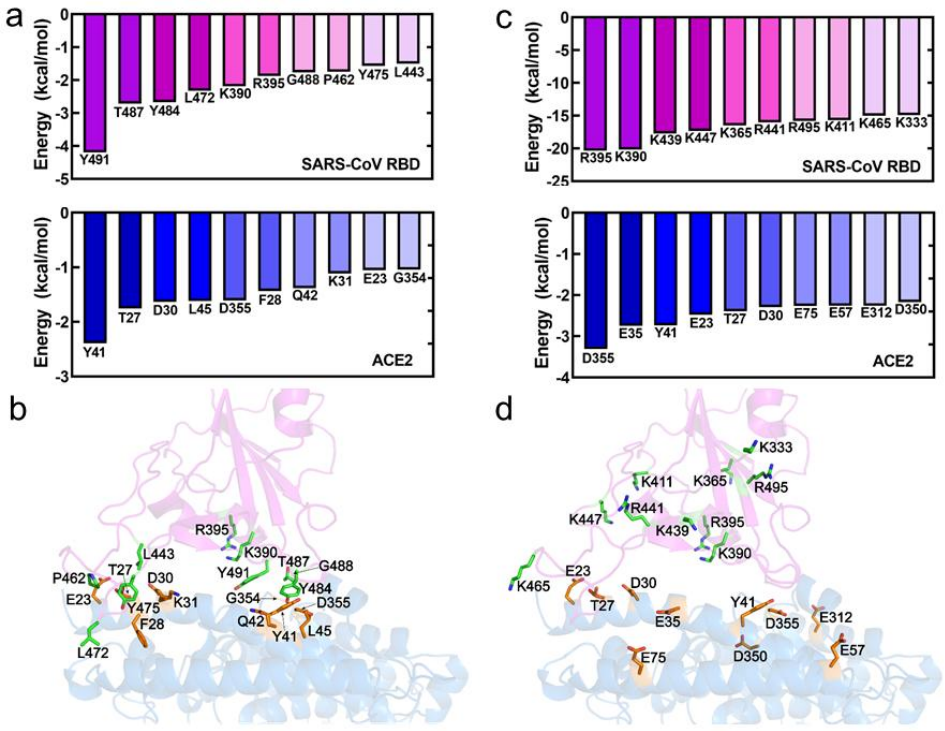

Figure S6. Decomposition of the energy per residue in the interaction between the RBD of SARS-CoV and ACE2. (a) The top-ten per-residue binding energy determined by the screening MM/PBSA (ε_{in}=2.0), most of the residues were near the binding site (b); (c) The top-ten per-residue binding energy determined by the standard MM/PBSA (ε_{in}=6.0), most of the residues were far away from the binding site (d).

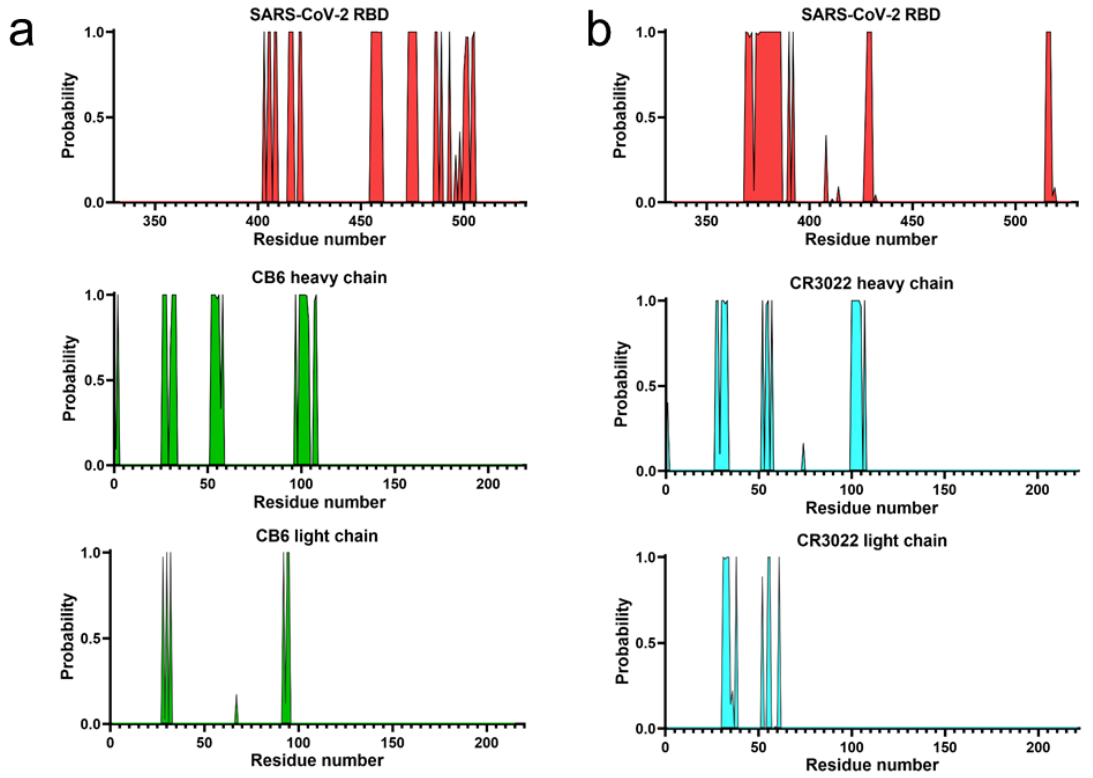

Figure S7. The contact probability of the residues in the SARS-CoV-2 RBD/CB6 interface (a) and SARS-CoV-2 RBD/CR3022 interface (b). The criterion for the residue contact is that the distance between two heavy atoms is smaller than 0.50 nm.

333 TNLCPFGEVFNATRFASVYAWNRKRISNCVADYSVLYNSASFSTFKCYGV **382**

383 SPTKLNDLCFTNVYADSFVIRGDEVRQIAPGQTGKIADYNYKLPDDFTGC **432**

433 VIAWNSNNLDSKVGGNYNYLYRLFRKSNLKPFERDISTEIYQAGSTPCNG **482**

483 VEGFNCYFPLQSYGFQPTNGVGYQPYRVVVLSFELLHAPATVCG **526**

Figure S8. The amino acid sequences of SARS-CoV-2 RBD. The contacting residues in the SARS-CoV-2 RBD/ACE2 interface are indicated by red fonts, the contacting residues in the SARS-CoV-2 RBD/CB6 interface are indicated by yellow background and the contacting residues in the SARS-CoV-2 RBD/CR3022 interface are indicated by cyan background.

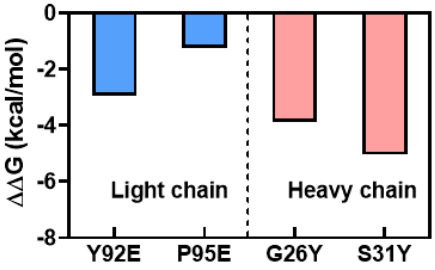

Figure S9. Some typical examples of residue mutation for enhancing the binding affinity ($\Delta\Delta G=\Delta G_{mutation}-\Delta G_{wild}$). Since the simple mutations cannot be applied, here the new trajectory of mutations was obtained by the simulations (i.e., rerunning the simulations after the mutation).

Table S1. The predicted binding free energy of SARS-CoV-2/ACE2 by using screening and standard MM/PBSA. All energy units are kcal/mol.

Method	ε_{in}	ΔE_{vdw}	ΔE_{ele}	ΔE_{pb}	ΔE_{sa}	ΔH	$-T\Delta S$	ΔG
Screening	2.0	-90.3±0.9	-99.3±2.9	167.4±2.4	-11.6±0.1	-33.7±1.4	20.4±2.2	-13.3±1.6
Standard	2.0	-90.3±0.9	-338.4±6.2	167.4±2.4	-11.6±0.1	-272.9±4.9	31.2±5.7	-241.7±3.1
	4.0	-90.3±0.9	-169.2±3.1	136.0±3.9	-11.6±0.1	-135.1±2.3	18.1±2.1	-117.0±3.0
	6.0	-90.3±0.9	-112.8±2.1	117.1±5.0	-11.6±0.1	-97.6±3.7	15.4±1.1	-82.2±3.1
	17.0	-90.3±0.9	-39.8±0.7	72.9±3.6	-11.6±0.1	-68.8±3.1	13.4±0.5	-55.4±2.7

Table S2. The predicted binding free energy of SARS-CoV/ACE2 by using screening and standard MM/PBSA. All energy units are kcal/mol.

Method	ε_{in}	ΔE_{vdw}	ΔE_{ele}	ΔE_{pb}	ΔE_{sa}	ΔH	$-T\Delta S$	ΔG
Screening	2.0	-86.2±1.7	-81.1±3.5	147.2±3.2	-11.7±0.1	-31.8±1.9	20.4±1.8	-11.4±1.4
Standard	2.0	-86.2±1.7	-329.5±4.2	147.2±3.2	-11.7±0.1	-280.2±3.1	28.9±4.8	-251.3±4.1
	4.0	-86.2±1.7	-164.7±2.1	127.3±2.5	-11.7±0.1	-135.4±0.9	15.3±2.4	-120.1±1.6
	6.0	-86.2±1.7	-109.8±1.4	111.9±2.3	-11.7±0.1	-95.8±0.9	11.8±1.4	-84.0±1.0

Table S3. The predicted binding free energy of SARS-CoV-2/CB6 by using screening and standard MM/PBSA. All energy units are kcal/mol.

Method	ε_{in}	ΔE_{vdw}	ΔE_{ele}	ΔE_{pb}	ΔE_{sa}	ΔH	$-T\Delta S$	ΔG
Screening	2.0	-114.1±1.1	-84.8±5.6	175.7±3.3	-14.0±0.1	-37.2±2.6	19.8±1.5	-17.4±3.2
Standard	2.0	-114.1±1.1	-71.4±5.4	175.7±3.3	-14.0±0.1	-23.8±5.1	23.0±1.0	-0.8±4.7
	4.0	-114.1±1.1	-35.7±2.7	136.0±3.0	-14.0±0.1	-27.8±4.3	16.2±1.2	-11.6±5.0
	6.0	-114.1±1.1	-23.8±1.8	113.4±2.9	-14.0±0.1	-38.5±4.2	15.1±1.8	-23.4±5.5

Table S4. The predicted binding free energy of SARS-CoV-2/CR3022 by using screening and standard MM/PBSA. All energy units are kcal/mol.

Method	ε_{in}	ΔE_{vdw}	ΔE_{ele}	ΔE_{pb}	ΔE_{sa}	ΔH	$-T\Delta S$	ΔG
Screening	2.0	-104.2±0.3	-162.7±3.2	245.5±2.5	-13.1±0.2	-34.5±2.6	23.2±1.4	-11.3±1.4
Standard	2.0	-104.2±0.3	-169.9±3.0	245.5±2.5	-13.1±0.2	-41.7±1.4	26.2±2.1	-15.5±1.1
	4.0	-104.2±0.3	-84.9±1.5	197.3±2.1	-13.1±0.2	-4.9±1.0	15.9±1.6	11.0±1.2
	6.0	-104.2±0.3	-56.6±1.0	168.1±1.8	-13.1±0.2	-5.8±1.0	14.9±1.5	9.1±1.5

Table S5. Computational alanine scanning determining the hot and warm spots in SARS-Cov-2 and CB6 by the screening MM/PBSA and IE method ($\Delta\Delta G=\Delta G_{ala}-\Delta G_{wild}$). All energy units are kcal/mol.

Mutation	$\Delta\Delta E_{vdw}$	$\Delta\Delta E_{ele}$	$\Delta\Delta E_{pb}$	$\Delta\Delta E_{sa}$	$\Delta\Delta H$	$-T\Delta\Delta S$	$\Delta\Delta G$
CB6 light chain							
S28A	0.33	0.41	-1.43	0.06	-0.63	-0.61	-1.24
S30A	0.54	0.54	-2.82	0.09	-1.65	0.53	-1.12
Y32A	4.03	0.37	-5.32	0.55	-0.37	-1.08	-1.44
Y92A	6.65	2.47	-9.02	0.42	0.52	-0.49	0.03
T94A	3.13	0.09	-2.22	0.19	1.18	-0.62	0.56
P95A	1.45	0.26	-0.34	0.10	1.47	0.21	1.67
CB6 heavy chain							
V2A	0.42	-0.01	0.60	-0.04	0.97	-0.80	0.17
F27A	0.81	-0.11	0.08	0.00	0.78	0.09	0.86
T28A	1.07	0.61	-2.17	0.09	-0.41	-0.18	-0.59
S30A	0.11	0.62	-0.72	0.00	0.01	-0.36	-0.35
S31A	1.06	-0.23	-1.86	0.04	-0.98	0.24	-0.75
N32A	0.68	0.79	1.16	-0.03	2.60	-0.88	1.72

Y33A	3.59	5.25	-7.73	0.00	1.11	0.33	1.45
Y52A	4.85	0.25	-6.71	0.20	-1.41	-0.99	-2.40
S53A	0.46	2.88	-1.58	0.02	1.78	-0.97	0.82
S56A	-1.36	6.56	-3.56	0.07	1.72	-0.56	1.16
F58A	2.94	0.48	-2.55	0.26	1.12	0.32	1.44
R97A	2.26	7.45	-3.48	0.01	6.24	0.09	6.33
L99A	2.71	0.16	-0.91	0.00	1.96	0.20	2.15
P100A	4.33	-0.53	1.51	-0.03	5.28	0.69	5.97
M101A	4.19	0.79	-1.57	0.23	3.71	-0.04	3.67
Y102A	2.15	0.79	-0.74	0.18	2.37	-0.49	1.88
D104A	0.38	16.48	-19.42	0.00	-2.56	-2.02	-4.58
D107A	0.65	1.45	-2.35	-0.01	-0.26	0.98	0.73
Y108A	1.08	0.03	0.00	0.05	1.17	0.02	1.19
SARS-CoV-2 RBD							
R403A	4.59	20.44	-18.97	0.36	6.41	-1.17	5.25
D405A	1.60	-8.67	-0.47	0.05	-7.50	2.05	-5.45
E406A	0.91	-7.13	-0.86	0.00	-7.09	0.23	-6.86
R408A	3.21	3.13	-1.77	0.41	4.98	-0.44	4.54
Q409A	1.24	0.73	-2.03	0.11	0.05	-0.36	-0.31
T415A	1.40	0.04	-1.67	0.09	-0.14	0.23	0.09
K417A	4.86	21.63	-31.91	0.57	-4.84	-1.27	-6.11
D420A	-1.03	15.23	-14.17	-0.04	-0.02	-0.06	-0.08
Y421A	4.43	0.91	-5.09	0.07	0.32	0.09	0.40
L455A	3.50	0.03	-0.48	-0.06	2.99	0.29	3.28
F456A	5.82	0.24	-3.47	0.20	2.80	-0.01	2.79
R457A	0.24	-3.06	2.84	0.00	0.01	-0.14	-0.13
K458A	2.13	-5.97	2.79	0.11	-0.95	0.96	0.01
S459A	0.04	-0.03	-0.10	0.00	-0.08	0.15	0.07
N460A	1.91	2.61	-4.65	0.04	-0.09	-0.51	-0.60
Y473A	1.89	3.82	-3.74	-0.04	1.92	0.12	2.04
Q474A	0.23	-0.55	0.68	0.00	0.35	0.07	0.43
S477A	0.22	0.18	-0.44	0.02	-0.02	0.08	0.06
F486A	4.42	1.85	-3.81	0.53	2.99	-0.27	2.72
N487A	0.85	9.41	-5.67	-0.01	4.58	-0.15	4.43
Y489A	5.15	1.26	-3.08	0.19	3.51	0.47	3.98
Q493A	4.15	3.44	-7.10	0.42	0.90	-0.38	0.52
T500A	0.11	0.02	0.04	0.00	0.17	0.24	0.41
N501A	0.75	1.53	-2.64	-0.01	-0.37	-0.10	-0.48
Y505A	3.96	-0.29	-1.95	0.17	1.89	0.09	1.99